

## Supporting Information

# **A new pyrimidine-amide-tetrazole ligand derived polyoxometalate-based copper complexes as catalysts for sulfide-sulfoxide transformation and electrochemical sensors**

**Jun-Jun Lu, Hong-Yan Lin, Qian-Qian Liu, Xiao-Dong Liu, Xiu-Li Wang\***

*College of Chemistry and Materials Engineering, Bohai University, Professional Technology Innovation Center of Liaoning Province for Conversion Materials of Solar Cell, Jinzhou 121013, P. R. China.*

### **X-ray Crystallographic Study**

The single-crystal X-ray diffraction data for complexes **1–2** were collected using a Bruker SMART APEX II with Mo K $\alpha$  radiation ( $\lambda = 0.71073 \text{ \AA}$ ) by  $\omega$  and  $\theta$  scan mode at room temperature. Both of the structures were solved by direct methods with the Olex2 software. The final refinement was performed by full matrix least-squares techniques on  $F^2$ . All non-hydrogen atoms were refined with anisotropic temperature parameters. All hydrogen atoms were placed in geometrically idealized position as a riding mode. The CCDC numbers are 2237491 and 2237492.

### **Synthesis of 4-H<sub>2</sub>pat ligand**

4-Pyrimidinecarboxylic acid (4g), 5-amino-1H-tetrazol (2.74g) and 50 ml of pyridine were added to a 250 ml distillation flask, and 10 ml of triphenyl phosphite was slowly added after stirring for 20 minutes. The mixture was refluxed for 10 h. The product was cooled at room temperature and stood for one day, then filtered and rinsed with ethanol to obtain a brown powder solid.

---

\* Corresponding author. Tel: +86-416-3400160

E-mail address: [wangxiuli@bhu.edu.cn](mailto:wangxiuli@bhu.edu.cn) (X.-L. Wang)

## Catalytic oxidation of sulfides

Complex **1** (3  $\mu\text{mol}$ ), 2mL of methanol solution, sulfide (0.5 mmol) and *tert*-butyl hydroperoxide (TBHP) (0.75 mmol) were added to the reaction glass tube and reacted at 50 °C for 45 min. The mixture was analyzed by gas chromatography (GC) every certain time.

## Preparation of the bulk-modified carbon paste electrodes with complexes **1** and **2** (1-2-CPEs)

The graphite nano-powder (0.1 g) and the complex **1** or **2** (0.015 g) were accurately weighed and mixed thoroughly with grinding in a mortar for 45 min, and an appropriate amount of paraffin oil was added dropwise to the ground powder and stirred to a paste-like mixture. The above substances were transferred to a glass tube with an inner diameter of 3 mm, compacted with a copper rod, and the electrode surface was polished to smooth with a weighing paper.

**Table. S1** Selected bond distances ( $\text{\AA}$ ) and angles ( $^\circ$ ) for complexes **1–2**.

Complex <b>1</b>			
Cu(1)-N(2)	1.974(7)	Cu(1)-N(1)	2.056(6)
Cu(1)-N(3)	2.026(6)	Cu(1)-O(1)	1.909(6)
Cu(1)-O(2)	2.198(5)	Cu(2)-O(1)	1.900(5)
Cu(2)-N(5)	1.987(6)	Cu(2)-N(6)	2.007(6)
Cu(2)-N(4)	1.998(6)	Cu(3)-O(2W)	1.943(6)
Cu(3)-O(4)	1.998(5)	Cu(3)-O(19)#1	2.271(6)
Cu(3)-N(9)#2	2.041(6)	Cu(3)-N(7)	1.936(6)
Cu(3)-O(3W)	2.339(7)	Cu(4)-O(1W)	1.959(6)
Cu(4)-N(13)#3	2.021(6)	Cu(4)-O(3)	1.953(5)
Cu(4)-N(8)	1.958(6)	Cu(4)-O(8)	2.509(5)
Cu(4)-O(20)	2.576(6)	N(2)-Cu(1)-N(1)	99.4(3)
N(2)-Cu(1)-N(3)	81.1(3)	N(2)-Cu(1)-O(2)	90.2(2)
N(1)-Cu(1)-O(2)	91.2(2)	N(3)-Cu(1)-N(1)	134.2(3)

N(3)-Cu(1)-O(2)	134.5(2)	O(1)-Cu(1)-N(2)	171.7(3)
O(1)-Cu(1)-N(1)	88.4(3)	O(1)-Cu(1)-N(3)	95.4(2)
O(1)-Cu(1)-O(2)	86.9(2)	N(4)-Cu(2)-N(6)	147.8(3)
N(5)-Cu(2)-N(4)	103.0(3)	N(5)-Cu(2)-N(6)	81.2(3)
O(1)-Cu(2)-N(4)	89.4(2)	O(1)-Cu(2)-N(6)	93.0(2)
O(1)-Cu(2)-N(5)	164.9(3)	O(2W)-Cu(3)-O(4)	88.3(2)
O(2W)-Cu(3)-O(19)#1	89.9(2)	O(2W)-Cu(3)-N(9)#2	90.2(2)
O(2W)-Cu(3)-O(3W)	92.3(3)	O(4)-Cu(3)-O(19)#1	98.5(2)
O(4)-Cu(3)-N(9)#2	177.8(3)	O(4)-Cu(3)-O(3W)	88.7(2)
O(19)#1-Cu(3)-O(3W)	172.5(2)	N(9)#2-Cu(3)-O(19)#1	83.1(2)
N(9)#2-Cu(3)-O(3W)	89.7(3)	N(7)-Cu(3)-O(2W)	174.9(3)
N(7)-Cu(3)-O(4)	87.8(2)	N(7)-Cu(3)-O(19)#1	87.4(2)
N(7)-Cu(3)-N(9)#2	93.8(2)	N(7)-Cu(3)-O(3W)	90.9(3)
O(1W)-Cu(4)-N(13)#3	88.8(2)	O(1W)-Cu(4)-N(8)	171.6(2)
O(3)-Cu(4)-O(1W)	87.7(2)	O(3)-Cu(4)-N(13)#3	174.7(3)
O(3)-Cu(4)-N(8)	87.8(2)	N(8)-Cu(4)-N(13)#3	96.1(2)
O(20)-Cu(4)-N(8)	95.1(2)	O(20)-Cu(4)-N(13)#3	87.9(2)
O(20)-Cu(4)-O(1W)	92.1(2)	O(20)-Cu(4)-O(3)	88.1(2)
O(8)-Cu(4)-O(1W)	87.3(2)	O(8)-Cu(4)-O(3)	90.3(2)
O(8)-Cu(4)-N(8)	85.3(2)	O(8)-Cu(4)-N(13)#3	93.5(2)

---

Symmetry code for **1**: #1 x, y+1, z; #2 x+1, y, z; #3 x-1, y, z

---

**Complex 2**

---

Cu(1)-O(2W)	1.945(5)	Cu(1)-N(2)	1.999(5)
Cu(1)-O(1W)	1.946(5)	Cu(1)-O(1)	2.498(5)
Cu(1)-N(1)	1.988(6)	Cu(2)-O(2)	1.915(5)
Cu(2)-N(5)#2	1.967(6)	Cu(2)-O(3W)	1.954(5)
Cu(2)-N(3)	1.940(6)	Cu(2)-N(4)#3	2.348(6)
O(2W)-Cu(1)-N(2)	98.4(2)	O(2W)-Cu(1)-O(1W)	89.4(2)
O(2W)-Cu(1)-O(1)	86.35(19)	O(2W)-Cu(1)-N(1)	178.5(2)

N(2)-Cu(1)-O(1)	93.12(19)	O(1W)-Cu(1)-N(2)	170.8(2)
O(1W)-Cu(1)-O(1)	92.2(2)	O(1W)-Cu(1)-N(1)	92.1(2)
N(1)-Cu(1)-N(2)	80.1(2)	N(1)-Cu(1)-O(1)	93.7(2)
O(2)-Cu(2)-N(5)#2	168.5(2)	O(2)-Cu(2)-O(3W)	82.8(2)
O(2)-Cu(2)-N(3)	87.6(2)	O(2)-Cu(2)-N(4)#3	102.1(2)
N(5)#2-Cu(2)-N(4)#3	87.5(2)	O(3W)-Cu(2)-N(5)#2	89.8(2)
O(3W)-Cu(2)-N(4)#3	97.0(2)	N(3)-Cu(2)-N(5)#2	99.1(2)
N(3)-Cu(2)-O(3W)	169.5(2)	N(3)-Cu(2)-N(4)#3	88.9(2)

Symmetry code for **2**: #2 -x+1, -y, -z+1; #3 x, -y+1/2, z+1/2

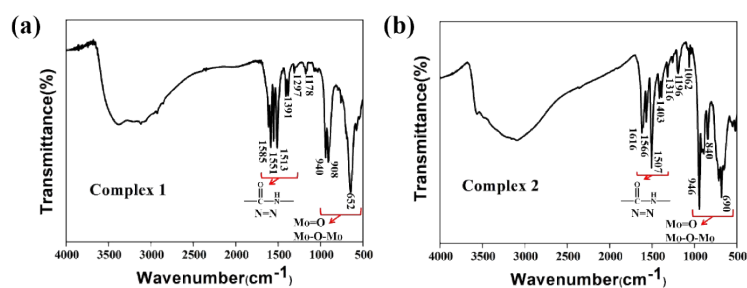


**Fig. S1.** (a-b) The IR spectra of complexes **1–2**.

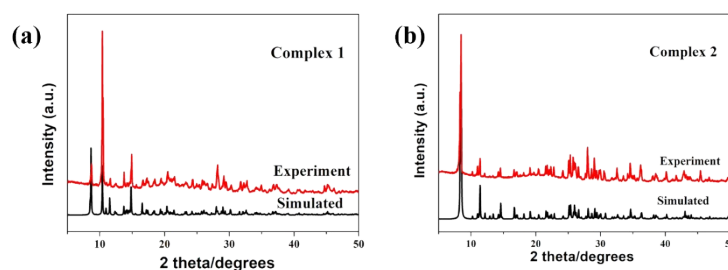


**Fig. S2.** (a-b) The PXRD patterns of complexes **1–2**.

**Table S2** Comparison of different POM-based catalysts for MPS oxidation.

Entry	Catalyst	Time (h)	Con.(%)	Ref.
1	Complex <b>1</b>	0.75	97	<b>This work</b>
2	Complex <b>2</b>	0.75	95	<b>This work</b>
3	$[\text{Ni}_3\text{L}_2(\text{CH}_3\text{OH})_6(\text{H}_2\text{O})_4][\text{PMo}_{12}\text{O}_{40}]_2 \cdot 3\text{CH}_3\text{OH} \cdot 2\text{H}_2\text{O}$	3	99	S1
4	$[\text{Ag}_3\text{L}(\text{PMo}_{12}\text{O}_{40})]$	1	92	S1

5	$(\text{Hbim})_2[\{\text{Cu}(\text{bim})_2(\text{H}_2\text{O})_2\}_2\{\text{Co}_2\text{Mo}_{10}\text{H}_4\text{O}_{38}\}]\cdot 5\text{H}_2\text{O}$	4	98	S2
6	$\text{H}_2[\text{Cu}(\text{dpdo})_3(\text{H}_2\text{O})_4][\{\text{Cu}_2(\text{dpdo})_3(\text{H}_2\text{O})_4(\text{CH}_3\text{CN})\}_2\{\text{Co}_2\text{Mo}_{10}\text{H}_4\text{O}_{38}\}_2]\cdot 9\text{H}_2\text{O}$	4	94	S2
7	$[\text{Zn}_{1.5}(\text{LOH})_3]\cdot (\text{PMo}_{12}\text{O}_{40})\cdot \text{CH}_3\text{OH}\cdot 2\text{H}_2\text{O}$	3	99	S3
8	$[\text{Ag}_4(\text{PMo}_{12}\text{O}_{40})(\text{L})_2]\cdot \text{OH}$	4	99	S4
9	$[\text{Ni}_2(1\text{-vIM})_7\text{H}_2\text{O}][\text{V}_4\text{O}_{12}]\cdot \text{H}_2\text{O}$	4	98	S5
10	$\text{Cu}_2(1\text{-vIM})_8[\text{V}_4\text{O}_{12}]\cdot \text{H}_2\text{O}$	4	98	S5

**Table S3** Catalytic oxidation of MPS by different catalysts under optimal conditions.

Entry	Catalyst	System	Time (min)	Con.(%)	Sel.(%)
1	Complex 1	heterogeneous	45	97	98
2	$\text{CrMo}_6$	homogeneous	45	71	99
3	$\text{CuCl}_2\cdot 2\text{H}_2\text{O}$	homogeneous	45	35	97
4	4- $\text{H}_2\text{pat}$	homogeneous	45	24	98
5	No catalyst	–	45	31	98

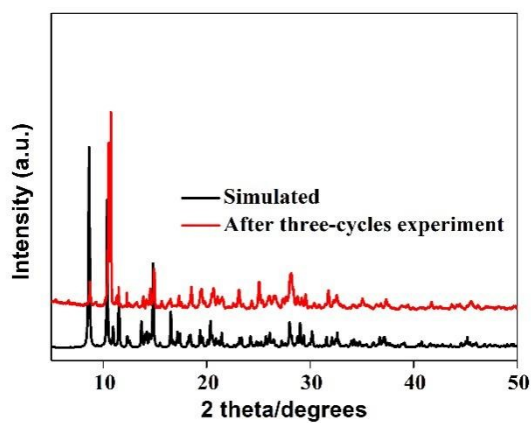


**Fig. S3.** The PXRD pattern of complex 1 after three-cycle experiments on the catalytic oxidation of MPS.

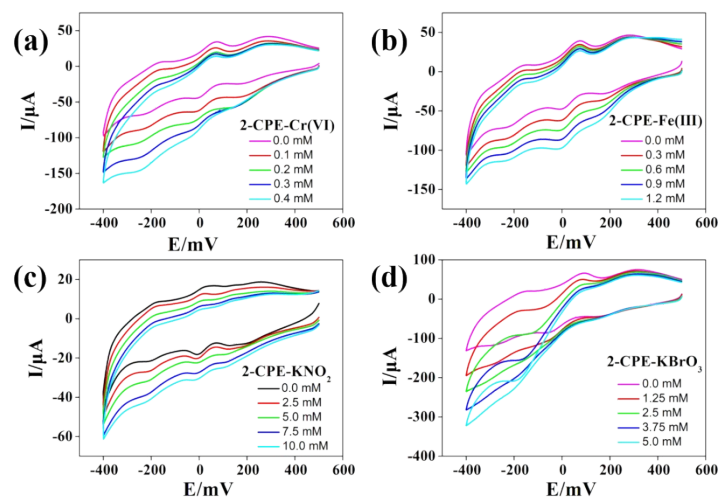


**Fig. S4.** The cyclic voltammograms of 2-CPE in 0.1 M  $\text{H}_2\text{SO}_4$  + 0.5 M  $\text{Na}_2\text{SO}_4$  electrolyte solution including (a) Cr(VI), (b) Fe(III), (c)  $\text{NO}_2^-$  and (d)  $\text{BrO}_3^-$  ions (scan rate:  $60 \text{ mV s}^{-1}$ ).

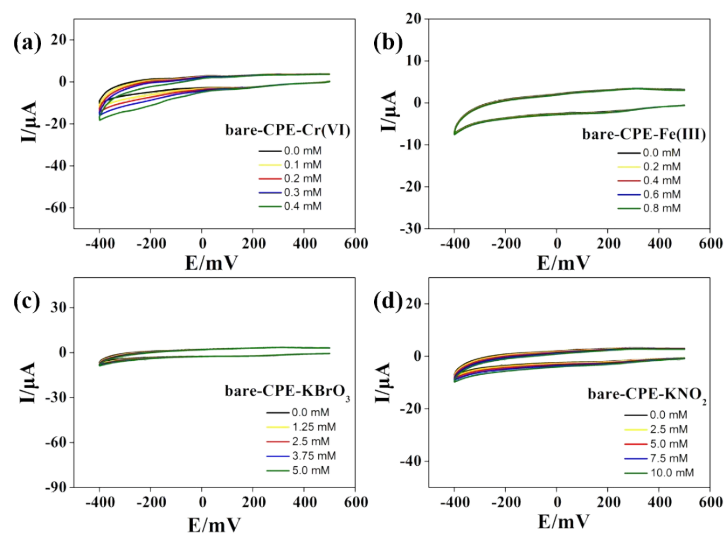


**Fig. S5.** The cyclic voltammograms of the bare-CPE in electrolyte solution containing Cr(VI), Fe(III),  $\text{BrO}_3^-$  and  $\text{NO}_2^-$ .

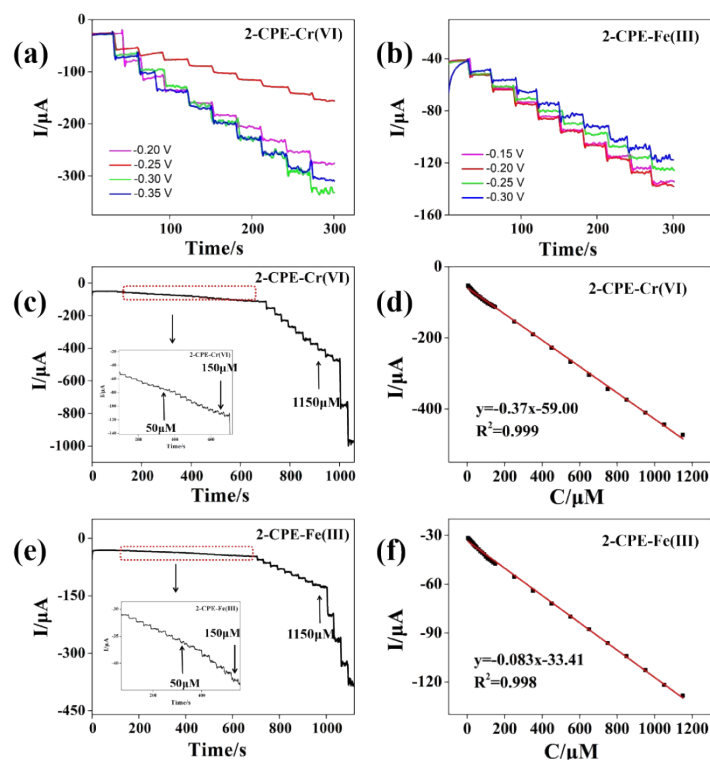


**Fig. S6.** The optimum potential of amperometric detection of (a) Cr(VI) and (b) Fe(III) for 2-CPE; (c) Current response of 2-CPE continuously adding different concentrations of Cr(VI); (d) The linear dependences between concentrations of Cr(VI) ions and redox peak currents for 2-CPE; (e) Current response of 2-CPE continuously adding different concentrations of Fe(III); (f) The linear dependences between concentrations of Fe(III) ions and redox peak currents for 2-CPE.

**Table S4** Parameters for Cr(VI) and Fe(III) determination using 1–2-CPEs.

		Detection limit ( $\mu\text{mol L}^{-1}$ )	Sensitivity ( $\mu\text{A } \mu\text{M}^{-1}$ )	Linear Range ( $\mu\text{mol L}^{-1}$ )
1-CPE	Cr(VI)	0.15	0.196	0.5-100
	Fe(III)	0.47	0.063	0.5-100
2-CPE	Cr(VI)	0.32	0.37	5-1150
	Fe(III)	1.44	0.083	5-1150

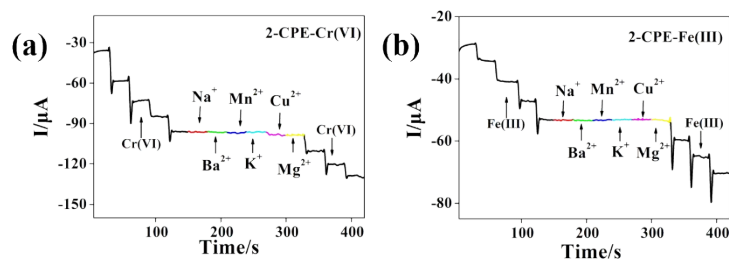


**Fig. S7.** Current response of 2-CPE varies with the addition of interfering metal ions ( $\text{Na}^+$ ,  $\text{Ba}^{2+}$ ,  $\text{Mn}^{2+}$ ,  $\text{K}^+$ ,  $\text{Cu}^{2+}$ ,  $\text{Mg}^{2+}$ ).

### Notes and references

- S1. J. Li, P. Du, Y. Y. Liu, J. F. Ma, *Dalton Trans.*, 2021, **50**, 1349.
- S2. H. Y. An, Y. J. Hou, L. Wang, Y. M. Zhang, W. Yang, S. Z. Chang, *Inorg. Chem.* 2017, **56**, 19, 11619.
- S3. Y. Q. Zhao, Y. Y. Liu, J. F. Ma, *Cryst. Growth Des.* 2021, **21**, 1019.
- S4. M. Y. Yu, T. T. Guo, X. C. Shi, J. Yang, X. X. Xu, J. F. Ma, Z. T. Yu, *Inorg. Chem.* 2019, **58**, 11010.
- S5. J. K. Li, C. P. Wei, D. G. J. Guo, C. C. Wang, Y. F. Han, G. F. He, J. P. Zhang, X. Q. Huang, C. W. Hu, *Dalton Trans.*, 2020, **49**, 14148.